

**Density-functional theory for one-dimensional harmonically trapped Bose-Fermi mixture**Hongmei Wang,<sup>1,2</sup> Yajiang Hao,<sup>3</sup> and Yunbo Zhang<sup>1,\*</sup><sup>1</sup>*Department of Physics and Institute of Theoretical Physics, Shanxi University, Taiyuan 030006, China*<sup>2</sup>*Department of Physics, Taiyuan Normal University, Taiyuan 030001, China*<sup>3</sup>*Department of Physics, University of Science and Technology Beijing, Beijing 100083, China*

(Received 19 March 2012; published 22 May 2012)

We present a density-functional theory for the one-dimensional harmonically trapped Bose-Fermi mixture with repulsive contact interactions. The ground-state density distribution of each component is obtained by solving the Kohn-Sham equations numerically based on the local density approximation and the exact solution for the homogeneous system given by Bethe ansatz method. It is shown that for sufficiently strong interaction, a considerable amount of fermions are repelled out of the central region of the trap, exhibiting partial phase separation of Bose and Fermi components. Oscillations emerge in the Bose density curves, reflecting the strong correlation with fermions. For infinitely strong interaction, the ground-state energy of the mixture and the total density are consistent with the scenario that all atoms in the mixture are fully fermionized.

DOI: [10.1103/PhysRevA.85.053630](https://doi.org/10.1103/PhysRevA.85.053630)

PACS number(s): 03.75.Mn, 71.15.Mb, 67.85.Pq

**I. INTRODUCTION**

Ultracold atomic gases provide a highly controllable testing ground to study fundamental problems in quantum many-body physics [1], and many experimental observations can be compared directly with exactly solvable theories. The degenerate quantum gases with many components in low spatial dimensions, especially in one dimension (1D), have become an increasingly interesting topic [2]. Multicomponent gases can be mixtures of the same species of atoms with different hyperfine states (i.e., spinor condensate) or mixtures of different species of atoms. The competition between the inter- and intraspecies interaction makes the mixture system more complicated and exhibit richer physical phenomena than its single-component counterpart. Bose-Fermi mixture is originally realized in experiments as a result of sympathetic cooling technique, that is, cooling the fermions to quantum degeneracy through the mediation of bosons [3–7]. Then many theoretical studies have been performed on three-dimensional mixtures, dealing with the phase separation [8], pairing [9], superfluid and Mott insulator transition [10], BEC and Bardeen-Cooper-Schrieffer (BCS) crossover [11], etc. On the other hand, 1D systems attract attention for the simplicity of theoretical models and for the significance of quantum correlation effects therein [12]. Experimentally the 1D systems can be realized by confining the cold atoms in two-dimensional optical lattices or in strong anisotropic magnetic traps [13]. The interaction among the atoms can be tuned in the whole regime of interaction strength via the magnetic Feshbach resonance and controlling the transverse confinement of the magnetic trap [14]. Interestingly enough, the properties of these system, including the ground-state, elementary excitations as well as thermodynamics, are sometimes fairly well captured by the exactly solvable models studied a few decades ago [15].

Many theories have studied 1D Bose-Fermi mixtures, both homogeneous and trapped gases in external potentials. When the system is homogeneous, Das [16] plots the ground-state phase diagram based on the mean-field theory, which predicts

the occurrence of phase separation (i.e., demixing) of the two components. Luttinger liquid formalism shows that for sufficiently strong repulsion the two components of the mixture, with bosons either a quasicondensate or impenetrable particles, repel each other sufficiently to demix [17]. However, the exact Bethe ansatz solution for the 1D mixture with equal mass and equal coupling constants points out the absence of demixing [18,19]. It indicates that mean-field theory and Luttinger liquid theory are reliable only for very weak interaction. With the system loaded in optical lattices, the phase diagram and correlation functions have been investigated with the bosonization method [20] and quantum Monte Carlo (MC) simulation [21]. For the trapped system, the local density approximation (LDA) on the Bethe ansatz solution shows that the harmonic trap 1D mixture would partially demix for strong repulsive interaction [19]. The finite temperature Yang-Yang thermodynamics and the quantum criticality analysis based on thermodynamic Bethe ansatz (TBA) both support the description of phase separation [22]. In the infinitely strong interaction limit, that is, the Tonks-Girardeau (TG) regime, the Bose-Fermi mapping method [23] shows that the density profiles display no demixing among the two components, where the exact ground state is highly degenerate and the most symmetrical one is chosen [24–26]. Later detailed calculations are done for all degenerate manifolds of the ground state [27], and the conclusion of nondemixing remains for the mixture in TG limit.

So far a method is not available for a 1D trapped Bose-Fermi mixture suitable for the whole repulsive interaction regime. However, numerical simulations such as the density matrix renormalization group (DMRG) and quantum MC are limited to a few atom numbers in lattice models [21,27]. In this paper, we develop a Hohenberg-Kohn-Sham density-functional theory (DFT) to investigate the ground-state properties of 1D harmonically trapped Bose-Fermi mixture. It is well known that DFT is a successful and widely used approach for treating electron systems with long-range Coulomb interaction [28,29]. Recently it has been successfully generalized to cold-atom systems with short-range contact interaction for three-dimensional bosonic atoms [30,31] and three-dimensional Bose-Fermi mixtures [32]. In the framework of DFT, in order

\*ybzhang@sxu.edu.cn

to investigate the ground-state properties of an inhomogeneous interacting system, a homogeneous interacting system is often needed in the process of LDA for the exchange correlation energy [28]. Because Bethe ansatz method can give exact solutions for 1D homogeneous systems, several authors developed the DFT based on Bethe ansatz results to solve the 1D bosons [31,33,34] and 1D Fermi cold-atom systems [35,36]. Here we apply this method for 1D Bose-Fermion mixture. As can be seen below, the key points of our scheme include a suitable fitting formula for the ground-state energy and appropriate choices of the functional orbitals for boson and fermions.

The paper is organized as follows. In Sec. II we derive the universal Kohn-Sham equations with LDA for a 1D Bose-Fermi mixture and then present the expression of exchange correlation energy. From the exact result of Bethe ansatz for homogeneous gas with equal masses of atoms and equal interaction of boson-boson and boson-fermion we find a fitting formula for the ground-state energy to simplify the numerical iterations. Then the equations are solved numerically and the ground-state energy and density distribution are discussed in Sec. III. Finally we conclude our result in the last section.

## II. THEORY

### A. Kohn-Sham equations

We consider a 1D trapped mixture of  $N_B$  bosons and  $N_F$  spin-polarized fermions with two-body contact interactions.  $N = N_B + N_F$  is the total atom number. The system is described by the Hamiltonian

$$\begin{aligned}
 H = & \sum_{i=1}^{N_B} \left[ -\frac{\hbar^2}{2m_B} \frac{d^2}{dx_i^2} + V_B(x_i) \right] \\
 & + \sum_{j=1}^{N_F} \left[ -\frac{\hbar^2}{2m_F} \frac{d^2}{dx_j^2} + V_F(x_j) \right] \\
 & + \frac{g_{BB}}{2} \sum_{i,i'=1}^{N_B} \delta(x_i - x_{i'}) + g_{BF} \sum_{i=1}^{N_B} \sum_{j=1}^{N_F} \delta(x_i - x_j).
 \end{aligned} \quad (1)$$

Here  $m_B$ ,  $m_F$  are boson and fermion masses,  $V_B(x)$ ,  $V_F(x)$  are external potentials, and  $g_{BB}$ ,  $g_{BF}$  are the effective 1D Bose-Bose and Bose-Fermi interaction parameters, which can be tuned experimentally [14,37]. The Fermi-Fermi interaction is not considered because the Pauli exclusion principle suppresses the contact  $s$ -wave scattering and their  $p$ -wave scattering can be neglected.

According to the Hohenberg-Kohn theorem I of DFT [28], the ground-state density of a bound system of interacting particles in some external potential determines this potential uniquely. It thus gives us the full Hamiltonian (1) and particle number  $N$ . Hence the density determines implicitly all properties derivable from  $H$  through the solution of the time-independent or time-dependent Schrödinger equation. Though proved originally for fermions, the theorem can be straightforwardly generalized to bosons as well as the mixture of bosons and fermions studied here. Denote the densities of bosons and fermions as  $n_B(x)$  and  $n_F(x)$ , respectively, and

the total density is then obviously  $n(x) = n_B(x) + n_F(x)$ . The number of bosons and fermions are conserved separately; that is,  $\int n_B(x)dx = N_B$ ,  $\int n_F(x)dx = N_F$  and  $\int n(x)dx = N$ . The ground-state energy, defined as  $\langle g|H|g \rangle$  with  $|g \rangle$  the ground state of system, is a functional of the densities  $E_0[n_B(x), n_F(x)]$ , which can be decomposed as

$$\begin{aligned}
 E_0 = & T_B^{\text{ref}}[n_B, n_F] + T_F^{\text{ref}}[n_B, n_F] \\
 & + \int dx n_B V_B(x) + \int dx n_F V_F(x) \\
 & + \frac{g_{BB}}{2} \int dx n_B^2(x) + g_{BF} \int dx n_B(x) n_F(x) \\
 & + E_{xc}[n_B, n_F].
 \end{aligned} \quad (2)$$

The first two terms are Bose and Fermi kinetic energies of a reference noninteracting system. The next two terms in the second row are external potential energies, and those in the third row are Hartree-Fock energies (i.e., the mean-field approximation of the interaction energy). The last term is the exchange correlation energy, which includes all the contributions to the interaction energy beyond mean-field theory.

We assume the bosons are in a quasicondensate state and fermions are in a normal state. Thus we introduce a single Bose functional orbital  $\phi(x)$  and  $N_F$  Fermi functional orbitals  $\psi_j(x)$  ( $j = 1, \dots, N_F$ ), which are orthogonal and normalized. This is different from the way of Ref. [38], where only one condensed orbital of fermionic pair is considered for the mixture of bosons and paired two-component fermions in a superfluid state or BCS state. With  $\phi(x)$  and  $\psi_j(x)$ , the densities are expressed as

$$n_B(x) = N_B \phi^*(x) \phi(x), \quad n_F(x) = \sum_{j=1}^{N_F} \psi_j^*(x) \psi_j(x). \quad (3)$$

and the kinetic energies are

$$T_B^{\text{ref}} = -N_B \int dx \phi^*(x) \frac{\hbar^2}{2m_B} \frac{d^2}{dx^2} \phi(x), \quad (4)$$

$$T_F^{\text{ref}} = -\sum_{j=1}^{N_F} \int dx \psi_j^*(x) \frac{\hbar^2}{2m_F} \frac{d^2}{dx^2} \psi_j(x). \quad (5)$$

As far as the exchange correlation energy  $E_{xc}[n_B, n_F]$  is concerned, when the confinement is weak, we adopt the LDA; that is, the system can be assumed locally homogeneous at each point  $x$  in the external trap. In this way  $E_{xc}$  is approximated with an integral over the exchange-correlation energy per atom of a homogeneous interacting mixture  $\varepsilon_{xc}^{\text{hom}}(n_B, n_F)$

$$E_{xc} \approx \int dx n(x) \varepsilon_{xc}^{\text{hom}}(n_B, n_F), \quad (6)$$

where the densities  $n_B$ ,  $n_F$  are taken at point  $x$ .

For such a homogeneous interacting mixture,

$$\varepsilon_{xc}^{\text{hom}} = \varepsilon^{\text{hom}} - \varepsilon_M^{\text{hom}} - \kappa_s^{\text{hom}}, \quad (7)$$

where  $\varepsilon^{\text{hom}}$  is the ground-state energy per atom;  $\varepsilon_M^{\text{hom}} = g_{BB} n_B^2 / 2n + g_{BF} n_B n_F / n$  is the mean-field interaction energy per atom;  $\kappa_s^{\text{hom}} = \hbar^2 \pi^2 n_F^3 / 6m_F n$  is the kinetic pressure terms, that is, the total kinetic energy dividing by the total number

of fermions and bosons in a noninteracting homogeneous mixture. Here the kinetic energy of the bosons is easily shown to be zero and the kinetic energy comes solely from the exclusive quantum state occupation of fermions.

Hohenberg-Kohn theorem II [28] guarantees that the ground-state density distributions are determined by variationally minimizing  $E_0$  with respect to  $n_B(x)$  and  $n_F(x)$ , which is equivalent to a variational calculation of Eq. (2) with respect to the Bose and Fermi functional orbitals  $\phi^*, \psi_j^*$ . After substituting Eq. (7) into Eq. (6) and substituting Eqs. (3)–(6) into Eq. (2), we carry out the functional derivatives

$$\begin{aligned} \delta \left( E_0 - \epsilon N_B \left( \int \phi^* dx \phi - 1 \right) \right) / \delta \phi^* &= 0, \\ \delta \left( E_0 - \sum_{j=1}^{N_F} \eta_j \left( \int \psi_j^* dx \psi_j - 1 \right) \right) / \delta \psi_j^* &= 0, \end{aligned} \quad (8)$$

where  $\epsilon$  and  $\eta_j$  ( $j = 1, 2, \dots, N_F$ ) are Lagrange multipliers conserving the normalization of  $\phi(x)$  and  $\psi_j(x)$ . Then we can get the Kohn-Sham equations (KSEs)

$$\left[ -\frac{\hbar^2}{2m_B} \frac{d^2}{dx^2} + V_B(x) + \mu_B^{\text{hom}}([n_B, n_F]; x) \right] \phi(x) = \epsilon \phi(x), \quad (9)$$

$$\begin{aligned} \left[ -\frac{\hbar^2}{2m_F} \frac{d^2}{dx^2} + V_F(x) - \frac{\hbar^2}{2m_F} \pi^2 n_F^2(x) \right. \\ \left. + \mu_F^{\text{hom}}([n_B, n_F]; x) \right] \psi_j(x) = \eta_j \psi_j(x). \end{aligned} \quad (10)$$

Here  $\mu_B^{\text{hom}} = \partial(n\epsilon^{\text{hom}})/\partial n_B$  and  $\mu_F^{\text{hom}} = \partial(n\epsilon^{\text{hom}})/\partial n_F$  are Bose and Fermi chemical potentials of a homogeneous interacting mixture. Physically  $\epsilon$  and  $\eta_j$  are the lowest eigenvalues of KSEs. In Eq. (3), the sum in  $n_F(x)$  runs over the occupied orbitals  $\psi_j$  with lowest  $\eta_j$ .

By left multiplying  $\psi_j^*$  on both sides of (10), performing summation over  $j$ , and integrating over  $x$ , we get an expression of  $T_F^{\text{ref}}$  defined in Eq. (5). Analogously from the normalization of  $\phi(x)$  we may get an expression for  $T_B^{\text{ref}}$  defined in Eq. (4). By inserting these two kinetic terms into Eq. (2), the ground-state energy (2) is expressed as a function of  $\epsilon$  and  $\eta_j$ :

$$\begin{aligned} E_0 &= N_B \epsilon + \sum_{j=1}^{N_F} \eta_j \\ &+ \int n(x) \epsilon^{\text{hom}}(x) dx - \int n_B(x) \mu_B^{\text{hom}}(x) dx \\ &- \int n_F(x) \mu_F^{\text{hom}}(x) dx + \frac{\hbar^2 \pi^2}{3m_F} \int n_F^3(x) dx. \end{aligned} \quad (11)$$

If  $\epsilon^{\text{hom}}[n_B, n_F]$  are known, we can solve the KSEs together with Eq. (3) to find the density distributions  $n_B(x)$ ,  $n_F(x)$  and then calculate the ground-state energy  $E_0$  from Eq. (11). In the following we present the result of  $\epsilon^{\text{hom}}[n_B, n_F]$  by means of the Bethe ansatz method.

### B. Ground-state energy of homogeneous system

In the absence of an external trap the system is homogeneous, which can be solved exactly via Bethe ansatz method

for a more restrictive but simple case:

$$g_{BB} = g_{BF} = g > 0, \quad m_B = m_F = m. \quad (12)$$

It describes the situation where the interactions of boson-boson and boson-fermion are repulsive with the same strength and the masses of boson and fermion are the same too. Detailed possible ways to realize this situation in cold-atom experiments have been considered previously [19]. The first condition can be satisfied using the combination of Feshbach resonance (to control the interactions) and appropriate choice of the tuning of the trapping laser frequencies (to adjust the the ratio of the radial confinement of bosons and fermions). The second condition is approximately satisfied with a mixture of two isotopes of a species of atoms. The isotope mixture is widely used in experiments because it can avoid the gravitational sag of an external potential caused by different masses. The experiments have realized three-dimensional (3D) isotope mixtures  $^6\text{Li}$ - $^7\text{Li}$  [4],  $^{173}\text{Yb}$ - $^{174}\text{Yb}$  [6],  $^{40}\text{K}$ - $^{41}\text{K}$  [7], and we see no obvious obstacles in 1D. Under these two conditions, the Hamiltonian of 1D homogeneous Bose-Fermi mixture is

$$H = -\frac{\hbar^2}{2m} \sum_{i=1}^N \frac{d^2}{dx_i^2} + g \sum_{i < j} \delta(x_i - x_j). \quad (13)$$

This model is solved by means of Bethe ansatz method by Lai and Yang in 1971 for the 1D mixture of bosons and spin- $\frac{1}{2}$  fermions [18]. Imambekov and Demler investigated the ground-state properties in detail for the 1D mixture of bosons and spin-polarized fermions [19], and extensive studies have been done [22,39–41], including the thermodynamics and correlation functions. Here we briefly review the main results of Refs. [18,19,41], which are readily used as the homogeneous reference system in our DFT theory. Under the periodic boundary condition and in the thermodynamical limit (the system size and the number of atoms are infinitely large but the atomic densities are kept finite), the ground-state Bethe ansatz integral equations are

$$\begin{aligned} \rho(k) &= \frac{1}{2\pi} \left[ 1 + \int_{-B}^B \frac{c\sigma(\Lambda)d\Lambda}{c^2/4 + (\Lambda - k)^2} \right], \\ \sigma(\Lambda) &= \frac{1}{2\pi} \int_{-Q}^Q \frac{c\rho(k)dk}{c^2/4 + (\Lambda - k)^2}, \end{aligned} \quad (14)$$

where  $c = mg/\hbar^2$ ,  $k$ , and  $\Lambda$  are the quasimomenta and spectral parameters and  $\rho(k)$  and  $\sigma(\Lambda)$  denote their corresponding density distributions. The integration limits  $B$  and  $Q$  are determined by the normalization condition

$$n_B = \int_{-B}^B \sigma(\Lambda)d\Lambda, \quad n = \int_{-Q}^Q \rho(k)dk. \quad (15)$$

The ground-state energy per atom is written in our notation as

$$\epsilon^{\text{hom}}(n_B, n_F, g) = \frac{1}{n} \int_{-Q}^Q \frac{\hbar^2 k^2}{2m} \rho(k)dk. \quad (16)$$

For convenience, let us define the fraction of bosons  $\alpha = n_B/n$  and the dimensionless Lieb-Liniger parameter  $\gamma = mg/(\hbar^2 n)$ . We then introduce variables  $x = k/Q$  and  $y = \Lambda/B$  such that  $\rho(k) = \rho(xQ) = g_c(x)$  and  $\sigma(\Lambda) = \sigma(yB) = g_s(y)$ , and Eqs. (14)–(16) are transformed into

$$g_c(x) = \frac{1}{2\pi} \left[ 1 + \frac{1}{\lambda_s} \int_{-1}^1 \frac{g_s(y)dy}{1/4 + (y/\lambda_s - x/\lambda_c)^2} \right], \quad (17)$$

$$g_s(y) = \frac{1}{2\pi} \frac{1}{\lambda_c} \int_{-1}^1 \frac{g_c(x)dx}{1/4 + (y/\lambda_s - x/\lambda_c)^2},$$

with

$$\lambda_c = \gamma \int_{-1}^1 g_c(x)dx, \quad \lambda_s = \frac{\gamma}{\alpha} \int_{-1}^1 g_s(y)dy, \quad (18)$$

and

$$\varepsilon^{\text{hom}}(n, \gamma, \alpha) = \frac{\hbar^2 n^2}{2m} e(\gamma, \alpha). \quad (19)$$

Here the function

$$e(\gamma, \alpha) = \frac{\gamma^3}{\lambda_c^3} \int_{-1}^1 x^2 g_c(x)dx \quad (20)$$

can be solved numerically with the combination of Eqs. (17) and (18) by the iteration method. In the limiting cases of  $\alpha = 0, 1$ , the system is purely fermions or purely bosons.  $e(\gamma, 0) = \pi^2/3$  is a constant while  $e(\gamma, 1)$  coincides with  $e_{\text{LL}}(\gamma)$  in the Lieb-Liniger model [42]. When the interaction is weak,  $\gamma \ll 1$ , the mean-field result of Eq. (19) is already available in Refs. [16, 19]; when the interaction is strong,  $\gamma \gg 1$ , one can neglect the dependence of the first integrand in Eq. (17) on  $x$  and  $g_c(x)$  can be approximated as a constant  $g_c$ . Therefore we get the asymptotic behavior of the function  $e(\gamma, \alpha)$  for  $\gamma$

$$e(\gamma \rightarrow 0, \alpha) = \frac{\pi^2}{3}(1 - \alpha)^3 + (2\alpha - \alpha^2)\gamma, \quad (21)$$

$$e(\gamma \rightarrow +\infty, \alpha) = \frac{\pi^2}{3} \left[ 1 - \frac{4F(\alpha)}{\gamma} + \frac{12F^2(\alpha)}{\gamma^2} \right],$$

where  $F(\alpha) = \alpha + \sin(\alpha\pi)/\pi$ . In the limiting case of  $\gamma = 0$ ,  $e(0, \alpha) = \pi^2(1 - \alpha)^3/3$ , and therefore  $\varepsilon^{\text{hom}}(n, 0, \alpha) = \hbar^2 \pi^2 n_F^3 / 6mn = \kappa_s^{\text{hom}}$ ; the energy comes solely from the kinetic energy of free fermions. In the Tonks-Girardeau limit,  $e(+\infty, \alpha) = \pi^2/3$ , which means the energy of Bose-Fermi mixture with infinitely strong repulsive interactions is equal to the energy of all atoms treated as free fermions.

For practical use, we need calculate  $e(\gamma, \alpha)$  for a lot of points  $(\gamma, \alpha)$ . If we use numeric iteration method for every point, it will be very time-consuming. To avoid this, we managed to retrieve a parametrization formula for  $e(\gamma, \alpha)$  based on the above limiting cases, which reads as

$$\tilde{e}(\gamma, \alpha) = \frac{\pi^2}{3}(1 - \alpha)^3 + f_1(\gamma)\{1 + f_2(\gamma)(1 - \alpha)^2 - [1 + f_2(\gamma)](1 - \alpha)^3\}. \quad (22)$$

Here  $f_1(\gamma)$  is the approximation of  $e_{\text{LL}}(\gamma)$ . We give

$$f_1(\gamma) = \frac{\pi^2}{3} \frac{\gamma^3 + a_2\gamma^2 + a_1\gamma}{\gamma^3 + b_2\gamma^2 + b_1\gamma + b_0} \quad (23)$$

with  $b_1 = 11.37, b_2 = 4.68, a_1 = 12 + b_1 - 4b_2, a_2 = -4 + b_2$ , and  $b_0 = \pi^2 a_1/3$ , which exhibits the same asymptotic behavior as  $e_{\text{LL}}(\gamma)$  in the weak and strong interaction cases to the order of  $\gamma$  and  $1/\gamma^2$ , respectively. The function  $f_2(\gamma)$  is determined by the numerical iteration result for some sampled values of  $\gamma$ , and we fit it as

$$f_2(\gamma) = c_0 \exp(c_1\gamma) - (c_0 + 1) \exp(c_2\gamma) \quad (24)$$

with  $c_0 = 0.21, c_1 = -0.02$ , and  $c_2 = -1.45$ .  $\tilde{e}(\gamma, \alpha)$  gives the exact behavior at the limits  $\alpha = 0, \gamma = 0, +\infty$  and approximates to  $e_{\text{LL}}(\gamma)$  at the limit  $\alpha = 1$ . In intermediate values of  $\alpha$  and  $\gamma$ ,  $\tilde{e}(\gamma, \alpha)$  deviates with a maximum relative error of 0.03 from the numerical result at  $\gamma \approx 2.5, \alpha \approx 0.9$ . In Fig. 1, we exhibit the result of exact numerical result of  $e(\gamma, \alpha)$  compared with the fitting formulas  $\tilde{e}(\gamma, \alpha)$  for various interaction strength  $\gamma$  and the fraction of bosons  $\alpha$ . Clearly the fitting formulas represent quite well the Betha-Ansatz result for the whole range of interaction and arbitrary fraction of bosonic atoms in the mixture. These formulas are then adopted in the following solution of the KSEs equations.

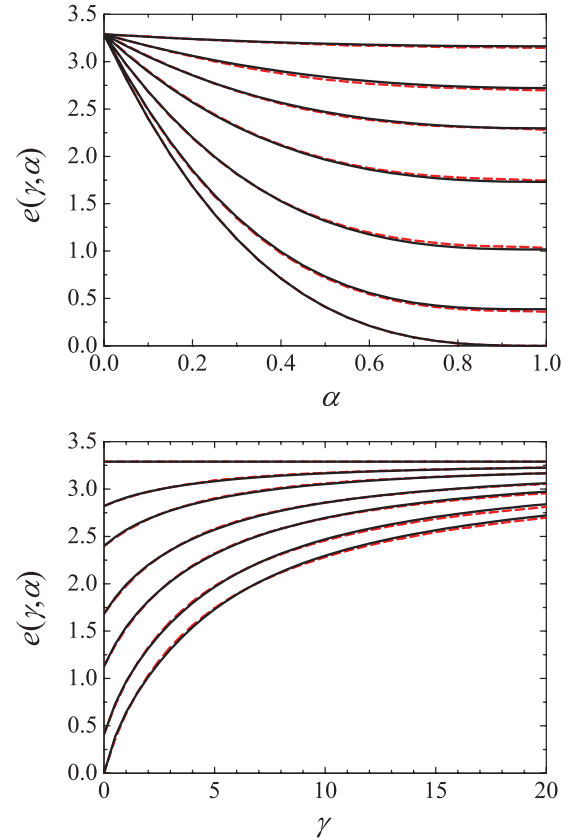


FIG. 1. (Color online) The function  $e(\gamma, \alpha)$  for the ground-state energy of homogeneous Bose-Fermi mixture system. Numerically exact result (red dashed line), obtained from the solution of Eqs. (17) and (18), is compared with the fitting formula (solid black line) given by Eq. (22). (a)  $\gamma = 0, 0.5, 2.5, 10, 20, 100$  from bottom to top; (b)  $\alpha = 0, 0.05, 0.1, 0.2, 0.3, 0.5, 1$  from top to bottom.

From  $\varepsilon^{\text{hom}}(n, \alpha, \gamma)$ , the ground-state Bose and Fermi chemical potentials can be obtained as

$$\begin{aligned}\mu_B^{\text{hom}}(n, \alpha, \gamma) &= \frac{\hbar^2 n^2}{2m} f_B(\gamma, \alpha), \\ \mu_F^{\text{hom}}(n, \alpha, \gamma) &= \frac{\hbar^2 n^2}{2m} f_F(\gamma, \alpha),\end{aligned}\quad (25)$$

where

$$\begin{aligned}f_B(\gamma, \alpha) &= 3e - \gamma \frac{\partial e}{\partial \gamma} + (1 - \alpha) \frac{\partial e}{\partial \alpha}, \\ f_F(\gamma, \alpha) &= 3e - \gamma \frac{\partial e}{\partial \gamma} - \alpha \frac{\partial e}{\partial \alpha},\end{aligned}\quad (26)$$

with  $f_B(0, \alpha) = 0$ ,  $f_F(0, \alpha) = \pi^2(1 - \alpha)^2$ , and  $f_B(+\infty, \alpha) = f_F(+\infty, \alpha) = \pi^2$ .

### III. NUMERICAL RESULTS

Inserting Eqs. (25) into the KSEs (9) and (10), and assuming bosons and fermions suffer from the same harmonic external potentials  $V_B(x) = V_F(x) = m\omega^2 x^2/2$ , with  $\omega$  is frequency, we can get the ground-state density profiles of each component by solving the KSEs together with the constraint (3) by means of numerical iteration. The ground-state energy follows immediately from Eq. (11). Here we introduce the length unit  $a = \sqrt{\hbar/m\omega}$  and a dimensionless interacting parameter  $U = g/a\hbar\omega$  such that the space-dependent Lieb-Liniger parameter is expressed as  $\gamma(x) = U/an(x)$ . Before going into the details of the DFT result, we first discuss the KSEs for some limiting cases.

When there is no interactions in the mixture,  $U = 0$ , KSEs correctly reduce to the equations for noninteracting bosons and noninteracting fermions in the harmonic trap. The densities of bosonic and fermionic components are respectively

$$n_B(x) = \frac{N_B}{a\sqrt{\pi}} \exp(-x^2/a^2), \quad (27)$$

$$n_F(x) = \frac{1}{a\sqrt{\pi}} \exp(-x^2/a^2) \sum_{l=0}^{N_F-1} \frac{H_l^2(x/a)}{2^l l!}, \quad (28)$$

where  $H_l(x)$  is the Hermite polynomials. Here the noninteracting Bose density profile (see the topmost black line in Fig. 2) is a standard Gaussian-like shape and Fermi density profile (see the red dotted line in Fig. 2) is characterized by a half-ellipse-like shape with  $N_F$  oscillations. The ground-state energies of these two components are

$$E_{0B} = \frac{N_B}{2} \hbar\omega, \quad (29)$$

$$E_{0F} = \sum_{l=0}^{N_F-1} \left( l + \frac{1}{2} \right) \hbar\omega, \quad (30)$$

and the total ground-state energy is  $E_0 = E_{0B} + E_{0F}$ .

When the interaction is weak, neglecting  $E_{xc}$  in Eq. (2), the KSEs reduce to our familiar mean-field formulas

$$\begin{aligned}\left[ -\frac{\hbar^2}{2m} \frac{d^2}{dx^2} + \frac{1}{2} m\omega^2 x^2 + g(n_B + n_F) \right] \phi &= \epsilon \phi, \\ \left[ -\frac{\hbar^2}{2m} \frac{d^2}{dx^2} + \frac{1}{2} m\omega^2 x^2 + gn_B \right] \psi_j &= \eta_j \psi_j.\end{aligned}\quad (31)$$

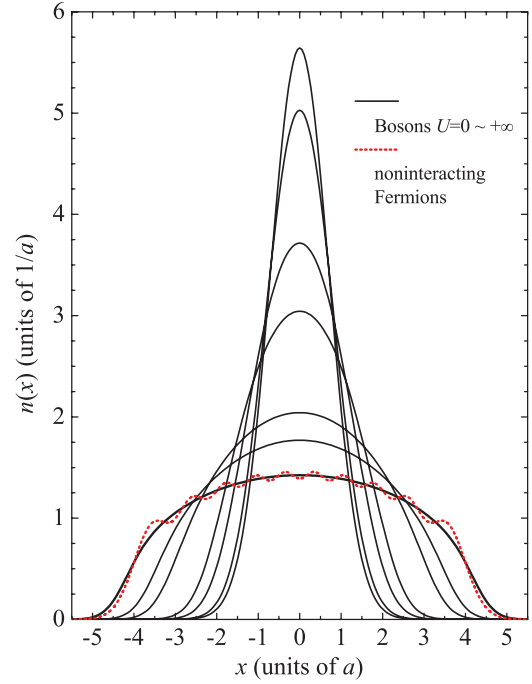


FIG. 2. (Color online) Density distribution of  $N_F = 10$  noninteracting fermions (red dotted line) and the density distributions of  $N_B = 10$  bosons for different interaction parameter  $U$ . The six black solid lines from top to bottom are respectively for bosons with  $U = 0, 0.1, 0.5, 1, 5, 10, +\infty$ .

For bosons it is nothing but the Gross-Pitaevskii equation for dilute gas. The equation for fermions, on the other hand, reminds us the superfluid theory of the mixture of bosons and paired BCS states of the two-component fermions where only one fermionic orbital is considered [38].

When the interaction is strong, for system of large atom numbers  $N_B, N_F \gg 1$ , one can safely use the Thomas-Fermi approximation (TFA), that is, the kinetic energies  $T_B^{\text{ref}}$  and  $T_F^{\text{ref}}$  in the energy functional (2) are approximated to zero and  $\int n(x) \kappa_s^{\text{hom}}(x) dx$ , respectively. Minimizing  $E_0$  directly with respect to  $n_B(x)$  and  $n_F(x)$ , we get the TFA formulas

$$\begin{aligned}\frac{1}{2} m\omega^2 x^2 + \mu_B^{\text{hom}}([N_B, N_F]; x) &= \mu_B^0, \\ \frac{1}{2} m\omega^2 x^2 + \mu_F^{\text{hom}}([N_B, N_F]; x) &= \mu_F^0,\end{aligned}\quad (32)$$

where  $\mu_B^0$  and  $\mu_F^0$  are constants fixed by the normalization conditions  $\int n_B(x) dx = N_B$  and  $\int n_F(x) dx = N_F$ . Equations (32) are explained as the LDA of the chemical potentials at point  $x$  in Ref. [19] and have been used extensively [22,40]. That means in slowly varying external harmonic trap chemical potentials at point  $x$  are related to those in the trap center  $x = 0$  ( $\mu_B^0$  and  $\mu_F^0$ ).

When repulsive interactions are infinitely strong,  $\mu_B^{\text{hom}} = \mu_F^{\text{hom}} = \hbar^2 \pi^2 n^2 / 2m$ , Eq. (32) reduces to a single equation:

$$\frac{1}{2} m\omega^2 x^2 + \frac{\hbar^2 \pi^2}{2m} n^2(x) = \mu^0, \quad (33)$$

with  $\mu^0$  is decided by  $\int n(x)dx = N$ . This gives us the explicit result for total density distribution

$$n(x) = \frac{\sqrt{2N - x^2/a^2}}{\pi a}, \quad (34)$$

and ground-state energy

$$E_0 = \frac{N^2}{2}\hbar\omega. \quad (35)$$

We see that they are exactly the density distribution and energy of  $N$  free fermions in a harmonic trap. Equation (33), however, gives nothing about the densities of Bose and Fermi components. The method here is insufficient for the infinitely strong interaction. We may, on the other hand, resort to the Bose-Fermi mapping method [23,24], which gives the Bose and Fermi density profiles as

$$n_{B,F}(x) = \frac{N_{B,F}}{N\sqrt{\pi}} \exp(-x^2/a^2) \sum_{n=0}^{N-1} \frac{H_n^2(x)}{2^n n!}. \quad (36)$$

The two components are nondemixing, in agreement with the generalized Bethe ansatz wave function [27],

The DFT results are summarized in Figs. 2–8. First, for a pure bosonic system, Eq. (9) is just the generalized Gross-Pitaevskii equation that appeared in Refs. [31,43]. We show the density profiles for  $N_B = 10$  bosons in Fig. 2 for the cases of  $U = 0, 0.1, 0.5, 1, 5, 10$ , and  $+\infty$ , respectively. With the increasing of  $U$ , the density profiles vary from a standard Gaussian-like to a nonoscillating half-ellipse shape. Comparing the density profiles of bosons at  $U = +\infty$  and the noninteracting fermions, we find that they match each other quite well except for the density oscillations. The results mean the density distribution of bosons with infinitely strong repulsive  $\delta$  interaction is basically the same as that of a noninteracting Fermi gas, which is consistent with Bose-Fermi mapping theory [44]. Our theory fails to reproduce the density oscillation due to the impenetrable property of 1D system with strong interaction because we adopt one single functional orbital  $\phi(x)$  for the 1D Bose liquid. The exact oscillations reflecting the structure of the occupied orbitals should be separated from the real wave function by the exact diagonalization method [45] or the reasonable analytical many-body wave function [46]. In the limit of large particle number, the differences between the oscillating and nonoscillating profiles become imperceptible.

The ground-state energy evolution as a function of  $U$  is illustrated in Fig. 3. We can see that with the increase of  $U$ , the kinetic energy  $T^{\text{ref}}$  decreases slowly, indicating that the interaction restrains the movement of atoms. The external potential energy  $E_{\text{pot}}$  increases as a result of wider occupied regime of the trap. Both of these two energies evolve to constant energies. The Hartree-Fock energy  $E_{\text{HF}}$  increases almost linearly while the exchange correlation energy  $E_{\text{xc}}$  decreases in the whole interaction regime. These two terms play more important roles in the DFT theory for stronger interaction and they approximately cancel each other. All these energies contribute to the total energy  $E_0$ , which starting from the noninteracting value  $5\hbar\omega$  approaches the strongly interacting limit  $50\hbar\omega$ . For  $U < 0.9$ , the exchange correlation energy is much less than the total energy,  $|E_{\text{xc}}/E_0| < 0.1$ ,

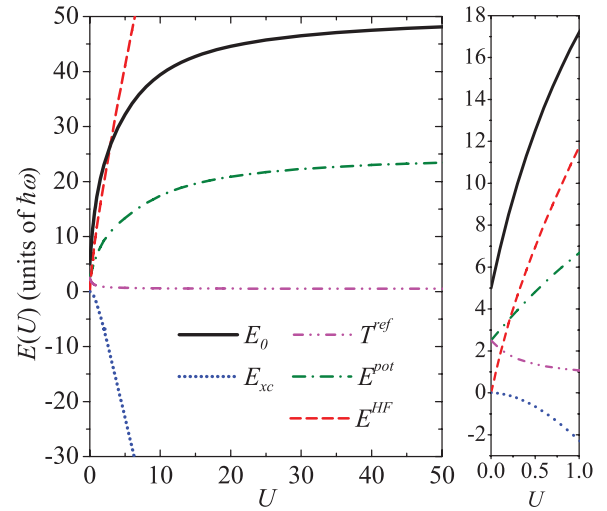


FIG. 3. (Color online) Evolution of energies of  $N_B = 10$  bosons with increasing interaction parameter  $U$ . Contributions to the ground-state energy  $E_0$  include kinetic energy  $T^{\text{ref}}$ , external potential energy  $E_{\text{pot}}$ , Hartree-Fock energy  $E_{\text{HF}}$ , exchange correlation energy  $E_{\text{xc}}$ . Right panel: Details in the mean-field regime.

which can be seen as the effective regime of mean field theory. For a TG gas with  $U = +\infty$  and a chemical potential  $\mu_B^{\text{hom}} = \hbar^2 \pi^2 n^2 / 2m$ , numerically solving equation (9) gives  $E_0 = 50.5024\hbar\omega$ , which lies slightly above  $50\hbar\omega$  because the introduced Bose functional orbital  $\phi(x)$  is only an assistant variational function instead of the true wave function of the interacting Bose system.

We now turn to illustrate the main result of a mixture of  $N_B = 10$  bosons and  $N_F = 10$  fermions. The densities of noninteracting mixtures (27) and (28) are taken as the starting point of the iteration of KSEs [Eqs. (9) and (10)] for a small interaction parameter (e.g.,  $U = 0.1$ ). The eigenvalues  $\epsilon, \eta_j$  and functional orbitals  $\phi, \psi_j$  are found by iterating to the desired degree of accuracy. The new densities are initial densities for the next iteration for a larger interaction parameter, and so on. The density profiles for different  $U$  are displayed in Fig. 4. It shows that with increasing  $U$ , the peak of the total density  $n(x)$  decreases monotonically and atoms tend to occupy wider regime. The density of the Fermi component changes smoothly in amplitude, while the Bose component becomes more flat and ripples begin to appear for stronger interaction. At weak interaction,  $U = 0.1, 1$  as in Figs. 4(a) and 4(b), both bosons and fermions are located in the center of the trap. For an intermediate interaction strength, for example,  $U = 5$  as in Fig. 4(c), some fermions are excluded from the center of the trap while bosons are held mainly in the center. We notice that oscillations emerge in the Bose density curves reflecting the strong correlation with fermions. When  $U$  becomes even stronger,  $U = 20, 100$  as in Figs. 4(d) and 4(e), more fermions are repelled from the center and a clear signature of phase separation of bosons and fermions is seen in the figures. High density of discrete bosons are surrounded by fermions, which nevertheless still have chance to squeeze between the opening space of bosons. The total density profile approaches a half-ellipse-like shape for  $U = +\infty$  as shown in Fig. 4(f). We may have a close inspection of the case of

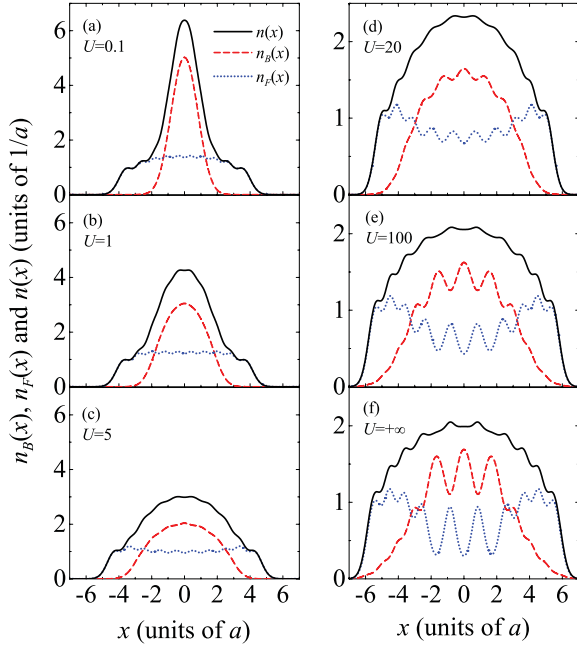


FIG. 4. (Color online) Density distributions of a mixture of  $N_B = 10$  bosons and  $N_F = 10$  fermions for different interaction parameter  $U = 0.1, 1, 5$  (left) and  $U = 20, 100, +\infty$  (right).

infinitely strong interaction. In Fig. 5, the DFT result of the total density is compared with those from TFA and Bose-Fermi mapping. It is clear that the agreement is fairly good except for tiny differences in the number, position, and amplitude of the oscillations, which are enlarged in the inset of Fig. 5. Again for large atom numbers the differences between the oscillating and nonoscillating curves are too small to be perceived.

Figure 6 describes the evolution of all contributed energy terms in Eq. (2) as a function of  $U$ . The line types denote the same energy terms as in Fig. 3 except that here the kinetic energy and external potential energy respectively include two terms relating to bosons (in red) and fermions (in blue). The trend of these lines resemble those in Fig. 3 for the same reason. In particular the exchange correlation energy here

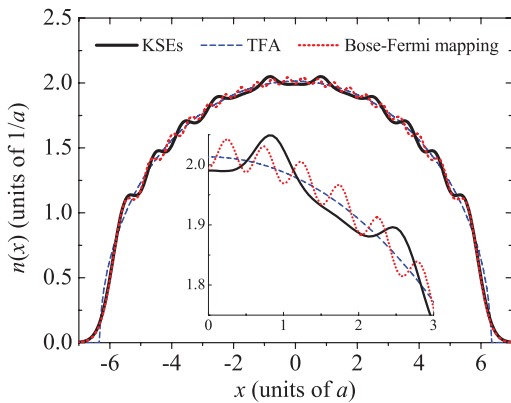


FIG. 5. (Color online) The total density profiles  $n$  as a function of  $x$  for a  $N_B = N_F = 10$  mixture with  $U = +\infty$ . The result of KSEs (black solid line), TFA (blue dashed line), and Bose-Fermi mapping (red dotted line) are compared, and the inset shows a zoom into the structure of the oscillations.

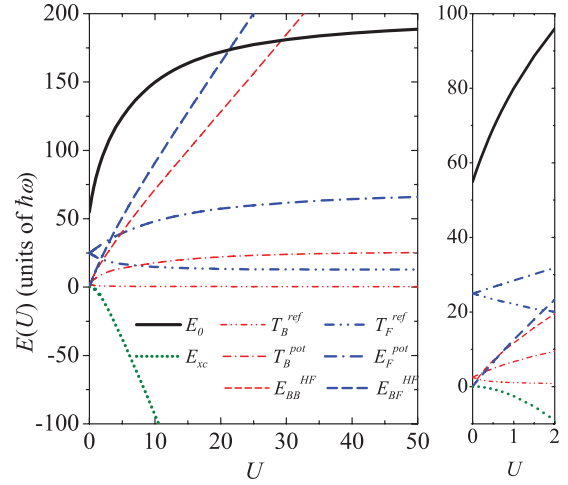


FIG. 6. (Color online) Ground-state energies as a function of  $U$  for mixture of  $N_B = N_F = 10$ . Contributions to the ground-state energy  $E_0$  are similar to those in Fig. 3. All terms but the exchange correlation energy originate from bosons and fermions. Right panel: Details in the mean-field regime.

contests with two Hartree-Fock terms representing the mean-field energy of boson-boson and boson-fermion interaction respectively. The total ground-state energy evolves from  $55\hbar\omega$ , the energy of 10 ideal bosons and 10 ideal fermions, to  $200\hbar\omega$ , the energy of 20 fully fermionized atoms according to Eqs. (29) and (30). In the parameter range of  $0 < U < 2$ ,  $|E_{xc}/E_0| < 0.1$ , mean-field theory is regarded effective. At  $U = +\infty$ , we numerically obtain an upper bound for the ground-state energy  $E_0 = 200.1364\hbar\omega$ , which is very close to the exact result of full fermionization  $E_0 = 200\hbar\omega$ .

There exist two contradicting predictions, phase separation and nondemixing, for the spatial structure of the components densities of trapped mixture in the TG limit. In Ref. [19] the authors use the Bethe-ansatz technique to prove that the mixture in the absence of external potential is always

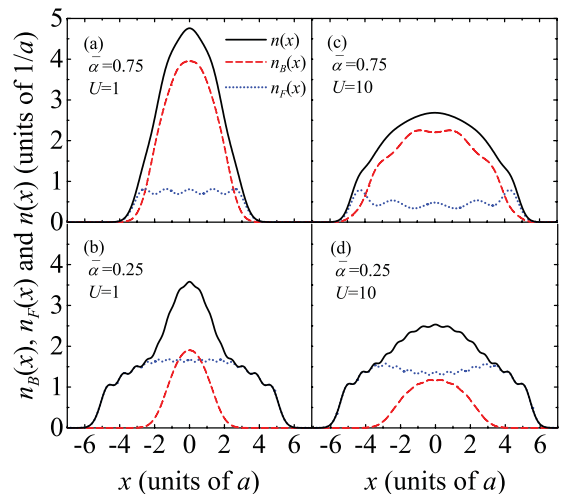


FIG. 7. (Color online) Density distributions of mixture with  $N = 20$  for different mean fractions of bosons  $\bar{\alpha} = N_B/N$  and different interaction parameters  $U$ .

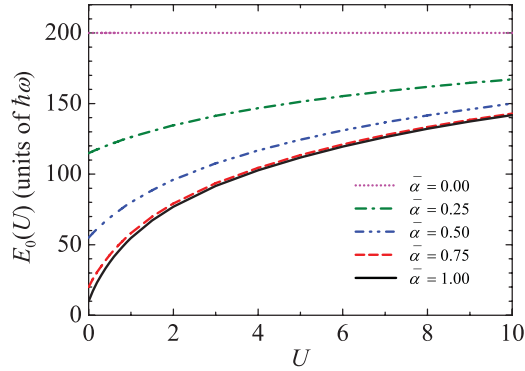


FIG. 8. (Color online) Ground-state energy  $E_0$  as a function of  $U$  for different fraction of bosons  $\bar{\alpha}$  in the mixture with total atom number  $N = 20$ .

stable against demixing, that is, bosons and fermions are mixed homogeneously showing no spatial structure. Then they combine the exact results of Bethe ansatz and TFA formulas (32) (where they called it LDA) to find the phase separation phenomenon for a harmonically trapped mixture with strong but finite interaction; for example, bosons and a small amount of fermions are present in the central part and the outer sections consist of fermions only. Both the thermodynamical Bethe ansatz (TBA) at finite temperature [22] and our DFT result for very strong and infinite repulsion as shown in Figs. 4(e) and 4(f) tend to support this scenario. The only difference is that the phase separation here is not complete: The bosons still have very few chances to occupy the outer Fermi sections. On the other hand, the nondemixing viewpoint is proposed with Bose-Fermi mapping methods for a TG mixture in Refs. [23,24], where it is shown that the component distributions of the  $N_B = N_F$  mixture are completely the same according to Eq. (36) and therefore display no demixing. However, the authors of Ref. [24] have noticed that the ground state given in this way is highly degenerate. They subsequently used a generalized Bethe ansatz wave function, in which the “orbital” part of the wave function is essentially replaced by a Slater determinant of a single-particle Schrödinger equation in the trap potential, to give a nondemixing result at finite large interactions. They further tested this nondemixing result with numerical DMRG simulations for a lattice model of  $N_B = N_F = 2$  mixture [27]. We observe, however, an obvious signature of phase separation in Fig. 4 of Ref. [27] for relatively large interaction  $U = 100$ . The intrinsic nature of the phase separation and nondemixing in the TG limit originates from the Bethe ansatz and Bose-Fermi mapping techniques respectively. We expect experimental verification of the nature of spatial configuration about trapped ultracold atomic mixtures.

Finally we discuss the effect of another system parameter, the mean value of the fraction of bosonic atoms number  $\bar{\alpha} = N_B/N$ , on the density profiles. Figure 7 shows the density of each component and the total density of  $N = 20$  atoms in the mixture with  $\bar{\alpha} = 0.25, 0.75$  and interaction parameters  $U = 1, 10$ . Figure 8 compares their energies. Bosons will dominate the total density profile when more bosons are put into the mixture for weak as well as strong interactions. When more fermions are prepared in the gas, bimodal distribution is clearly seen the total density where bosonic Gaussian shape is superimposed onto the fermionic shell-like structure. In the strong interaction limit the total density approaches the typical half-ellipse no matter how many bosons or fermions are involved in the mixture. The number of fermions contribute to the ground-state energy more effectively in the weak interaction case. This situation changes for strong interaction where the energies for all values of  $\bar{\alpha}$  approximate to the limit value of the full fermionization of the system.

#### IV. CONCLUSION

In conclusion, using the DFT we study the ground-state energy and density distribution of the Bose-Fermi mixture in a quasi-1D harmonic trap. Based on the Bethe ansatz solution for the mixture, we managed to obtain a fitting formula for the function  $e(\gamma, \alpha)$  for the ground-state energy of homogeneous system. The KSEs are obtained from the variational minimization of the energy functional of the trapped mixture with respect to the densities of Bose and Fermi components. We found that when the interaction between the atoms varies from zero to positive infinitely, the ground-state energy of the mixture would evolve to the constants of the noninteracting fermions and the total density approached a half-ellipse profile. More fermions are repelled out of the trap center, while bosons occupy the central region. Phase separation of boson and fermion components occurs for strong interaction in agreement with the the result Bethe ansatz method plus LDA. The calculation here applies equally to the pure bosonic case, different fraction of bosons, as well as in the TG limit. Our DFT theory is also suitable for mixtures in optical lattice and could be extended to study the dynamical and thermodynamic phenomena of the mixture.

#### ACKNOWLEDGMENTS

This work is supported by the NSF of China under Grants No. 11104171 and No. 11074153, the National Basic Research Program of China (973 Program) under Grants No. 2010CB923103 and No. 2011CB921601, the NSF of Shanxi Province, and the Program for New Century Excellent Talents in University (NCET). We thank Gao Xianlong for helpful discussions.

- [1] C. J. Pethick and H. Smith, *Bose-Einstein Condensation in Dilute Gases*, 2nd ed. (Cambridge University Press, New York, 2008).
- [2] M. A. Cazalilla, R. Citro, T. Giamarchi, E. Orignac, and M. Rigol, *Rev. Mod. Phys.* **83**, 1405 (2012).

- [3] B. DeMarco and D. S. Jin, *Science* **285**, 1703 (1999).
- [4] A. G. Truscott, K. E. Strecker, W. I. McAlexander, G. B. Partridge, and R. G. Hulet, *Science* **291**, 2570 (2001).
- [5] G. Modugno, G. Ferrari, G. Roati, R. J. Brecha, A. Simoni, and M. Inguscio, *Science* **294**, 1320 (2001); G. Modugno, G. Roati,



- F. Riboli, F. Ferlaino, R. J. Brecha, and M. Inguscio, *ibid.* **297**, 2240 (2002); S. Ospelkaus, C. Ospelkaus, O. Wille, M. Succo, P. Ernst, K. Sengstock, and K. Bongs, *Phys. Rev. Lett.* **96**, 180403 (2006).
- [6] T. Fukuhara, S. Sugawa, Y. Takasu, and Y. Takahashi, *Phys. Rev. A* **79**, 021601 (2009).
- [7] C.-H. Wu, I. Santiago, J. W. Park, P. Ahmadi, and M. W. Zwierlein, *Phys. Rev. A* **84**, 011601(R) (2011).
- [8] K. Mølmer, *Phys. Rev. Lett.* **80**, 1804 (1998).
- [9] M. Lewenstein, L. Santos, M. A. Baranov, and H. Fehrmann, *Phys. Rev. Lett.* **92**, 050401 (2004).
- [10] F. Hebert, F. Haudin, L. Pollet, and G. G. Batrouni, *Phys. Rev. A* **76**, 043619 (2007).
- [11] F. Illuminati and A. Albus, *Phys. Rev. Lett.* **93**, 090406 (2004).
- [12] T. Giamarchi, *Quantum Physics in One Dimension* (Oxford University Press, Oxford, 2004).
- [13] T. Kinoshita, T. Wenger, and D. S. Weiss, *Science* **305**, 1125 (2004); B. Paredes, A. Widera, V. Murg, O. Mandel, S. Fölling, I. Cirac, G. V. Shlyapnikov, T. W. Hänsch, and I. Bloch, *Nature (London)* **429**, 277 (2004).
- [14] M. Olshanii, *Phys. Rev. Lett.* **81**, 938 (1998).
- [15] B. Sutherland, *Beautiful Models: Seventy Years of Exactly Solved Quantum Many-Body Problems* (World Scientific, Singapore, 2004).
- [16] K. K. Das, *Phys. Rev. Lett.* **90**, 170403 (2003).
- [17] M. A. Cazalilla and A. F. Ho, *Phys. Rev. Lett.* **91**, 150403 (2003).
- [18] C. K. Lai and C. N. Yang, *Phys. Rev. A* **3**, 393 (1971).
- [19] A. Imambekov and E. Demler, *Phys. Rev. A* **73**, 021602(R) (2006); *Ann. Phys.* **321**, 2390 (2006).
- [20] L. Mathey, D. W. Wang, W. Hofstetter, M. D. Lukin, and E. Demler, *Phys. Rev. Lett.* **93**, 120404 (2004); L. Mathey and D. W. Wang, *Phys. Rev. A* **75**, 013612 (2007).
- [21] Y. Takeuchi and H. Mori, *Phys. Rev. A* **72**, 063617 (2005); P. Sengupta and L. P. Pryadko, *Phys. Rev. B* **75**, 132507 (2007); L. Pollet, M. Troyer, K. Van Houcke, and S. M. A. Rombouts, *Phys. Rev. Lett.* **96**, 190402 (2006).
- [22] X. Yin, S. Chen, and Y. Zhang, *Phys. Rev. A* **79**, 053604 (2009); X. Yin, X.-W. Guan, Y. Zhang, and S. Chen, *ibid.* **85**, 013608 (2012).
- [23] M. D. Girardeau and A. Minguzzi, *Phys. Rev. Lett.* **99**, 230402 (2007).
- [24] B. Fang, P. Vignolo, C. Miniatura, and A. Minguzzi, *Phys. Rev. A* **79**, 023623 (2009).
- [25] K. Lelas, D. Jukić, and H. Buljan, *Phys. Rev. A* **80**, 053617 (2009).
- [26] X. Lü, X. Yin, and Y. Zhang, *Phys. Rev. A* **81**, 043607 (2010).
- [27] B. Fang, P. Vignolo, M. Gattobigio, C. Miniatura, and A. Minguzzi, *Phys. Rev. A* **84**, 023626 (2011).
- [28] P. Hohenberg and W. Kohn, *Phys. Rev.* **136**, B864 (1964); W. Kohn and L. J. Sham, *ibid.* **140**, A1133 (1965); W. Kohn, *Rev. Mod. Phys.* **71**, 1253 (1999).
- [29] R. M. Dreizler and E. K. U. Gross, *Density Functional Theory* (Springer, Berlin, 1990).
- [30] G. S. Nunes, *J. Phys. B* **32**, 4293 (1999); A. Banerjee and M. P. Singh, *Phys. Rev. A* **73**, 033607 (2006); N. Argaman and Y. B. Band, *ibid.* **83**, 023612 (2011).
- [31] Y. E. Kim and A. L. Zubarev, *Phys. Rev. A* **67**, 015602 (2003).
- [32] A. P. Albus, F. Illuminati, and M. Wilkens, *Phys. Rev. A* **67**, 063606 (2003).
- [33] J. Brand, *J. Phys. B* **37**, S287 (2004).
- [34] Y. Hao and S. Chen, *Phys. Rev. A* **80**, 043608 (2009).
- [35] G. E. Astrakharchik, D. Blume, S. Giorgini, and L. P. Pitaevskii, *Phys. Rev. Lett.* **93**, 050402 (2004); Y. E. Kim and A. L. Zubarev, *Phys. Rev. A* **70**, 033612 (2004); R. J. Magyar and K. Burke, *ibid.* **70**, 032508 (2004).
- [36] G. Xianlong, M. Polini, R. Asgari, and M. P. Tosi, *Phys. Rev. A* **73**, 033609 (2006); G. Xianlong and R. Asgari, *ibid.* **77**, 033604 (2008).
- [37] M. Rizzi and A. Imambekov, *Phys. Rev. A* **77**, 023621 (2008).
- [38] S. K. Adhikari, B. A. Malomed, L. Salasnich, and F. Toigo, *Phys. Rev. A* **81**, 053630 (2010).
- [39] H. Frahm and G. Palacios, *Phys. Rev. A* **72**, 061604(R) (2005).
- [40] X.-W. Guan, M. T. Batchelor, and J.-Y. Lee, *Phys. Rev. A* **78**, 023621 (2008).
- [41] Y. Hao, *Chin. Phys. Lett.* **28**, 010302 (2011).
- [42] E. H. Lieb and W. Liniger, *Phys. Rev.* **130**, 1605 (1963).
- [43] E. B. Kolomeisky, T. J. Newman, J. P. Straley, and X. Qi, *Phys. Rev. Lett.* **85**, 1146 (2000); V. Dunjko, V. Lorent, and M. Olshanii, *ibid.* **86**, 5413 (2001); P. Öhberg and L. Santos, *ibid.* **89**, 240402 (2002).
- [44] M. Girardeau, *J. Math. Phys.* **1**, 516 (1960).
- [45] F. Deuretzbacher, K. Bongs, K. Sengstock, and D. Pfannkuche, *Phys. Rev. A* **75**, 013614 (2007).
- [46] I. Brouzos and P. Schmelcher, *Phys. Rev. Lett.* **108**, 045301 (2012).